Hydrophobic Shell Loading of PB-*b*-PEO Vesicles

Waltraut Mueller,[†] Kaloian Koynov,[‡] Karl Fischer,[†] Sonngard Hartmann,[†] Sebastien Pierrat,[†] Thomas Basché,[†] and Michael Maskos*,[†]

Institute of Physical Chemistry, University Mainz, Welder Weg 11, D-55128 Mainz, Germany, and Max-Planck-Institute of Polymer Research, D-55021 Mainz, Germany

Received August 28, 2008; Revised Manuscript Received November 17, 2008

ABSTRACT: We report on the successful encapsulation of hydrophobic substrates into the hydrophobic shell of poly(butadiene)-*b*-poly(ethylene oxide) vesicles in water and straightforward characterization methods. The hydrophobic fluorescent dye Nile Red was embedded into unilamellar vesicles of PB_{130}-*b*-PEO_{66} prepared via different methods leading to different average hydrodynamic radii and distributions but a common hydrophobic shell thickness of ∼16 nm as determined by transmission electron microscopy (TEM). The combination of cryogenic TEM and fluorescence microscopy studies shows that the self-assembled structure remains unchanged when the hydrophobic dye is incorporated within the vesicle shell. Furthermore, highly fluorescent quantum dots with an average diameter of $d = 5.7 \pm 0.6$ nm as determined by TEM were selected as hydrophobic model substrates and successfully enclosed into the vesicles, as evidenced by fluorescence correlation spectroscopy (FCS) measurements in combination with dynamic light scattering (DLS). Cryogenic TEM imaging reveals the position of the quantum dots, centered inside the double layer of the vesicle shell.

Introduction

Amphiphilic block copolymers tend to self-assemble in selective solvents like water. Depending on parameters like overall average molecular weight, volume fraction of each block, or effective interaction energy between monomers in the blocks, vesicles with bilayer shell and solvent interior volume similar to liposomes can be formed.[1] Such block copolymer vesicles in aqueous media have attracted increasing interest due to their enhanced stability compared to classical liposomes and due to the potential to control vesicle properties like bilayer thickness, permeability, or surface functionalities by appropriate chemical copolymer adjustment.[2]

The block copolymer polybutadiene-*block*-poly(ethylene oxide) (PB-*b*-PEO) is a frequently studied system under this aspect[3−6] as it offers several advantages. For example, the PEO that forms the surface of the assembled structures in water is in general regarded as biocompatible.[7,8] Furthermore, depending on the PB block length, the assembled vesicles can exhibit a thicker hydrophobic membrane core and therefore higher stability compared to liposomes.[9] Additionally, this copolymer features the possibility to cross-link the PB part and thereby stabilize the assembled structure.[10−12]

Drug delivery is mainly based on successful encapsulation of substrates with different solubility parameters. Micellar structures are favored in case of hydrophobic substrates solubilized within the hydrophobic core of the micelle.[13,14] Hydrophilic substrates are typically encapsulated by solubilization within the water-filled cavity of liposomes or vesicles. The hydrophilic vesicles core loading has been successful for several polymer systems including the PB-*b*-PEO system.[15,16] The hydrophobic encapsulation into the vesicle shell of various polymer systems has been reported recently,[17−23] but most of these works address the interface by simply utilizing amphiphilic substrates itself.[24−26] Reference 19, for example, demonstrates the usefulness of porphyrin-based fluorophores to study the influence of the dye size in comparison to the membrane thickness. A decrease in fluorescence intensity with increasing fluorophore concentration was observed and attributed to energy transfer to dark trap sites. However, it has not yet been possible to verify the fully hydrophobic nature of the encapsulation, especially in the case of colloidal substrates.

Thinking about potential pharmaceutical applications, encapsulation of different substrates at the same time is a demand but also a scientific challenge.[27] The vesicular system presented here offers the possibility for encapsulation of both hydrophilic and hydrophobic particles at the very same time in the very same particle. Potential loading systems are typically limited by the lack of suitable characterization methods. We utilized fluorescence correlation spectroscopy in combination with cryogenic TEM imaging and dynamic light scattering to characterize hydrophobic loading properties.

In order to understand the influence of different molecular parameters on structure formation and stability, we here report on the directed encapsulation of two hydrophobic model substrates inside the vesicle shell that both comply with requirements like water insolubility and sufficient fluorescence intensities for monitoring: Nile Red, a lipophilic fluorescent dye representing the molecular size regime,[28] and fluorescent CdSe/CdS/ZnS core/shell quantum dots, which carry hydrophobic surface ligands and serve as a model substrate of the nano size regime.[29,30]

Experimental Section

Materials. All vesicle solutions were produced in purified water (Waters Milli-Q system) and tetrahydrofuran (THF, uvasol grade, Riedel-de Haën, destabilized by distillation). The fluorescent dye Nile Red (structure, see Supporting Information) was used without purification (99%, Acros). Linear polybutadiene was purchased from Aldrich with $M_n = 1.53-2.07$ kg/mol.

The synthesis of poly(butadiene)-*b*-poly(ethylene oxide) was published before.[6] The copolymer PB_{130}-*b*-PEO_{66}-COOK was characterized by MALDI-TOF mass spectrometry, resulting in $M_n = 11$ kg/mol, $M_w/M_n = 1.05$, and 29% w/w PEO (the indices represent the number-average degree of polymerization of the individual blocks as determined by ^{1}H NMR).

The quantum dots consisting of a CdSe core capped with four monolayers CdS and one ZnS shell were synthesized according to the literature,[29,30] with oleic acid/oleyl amine as ligands and chloroform as final solvent. Characterization in toluene resulted in an absorption maximum at $\lambda = 586$ nm and an emission maximum

* Corresponding author. E-mail: maskos@uni-mainz.de.
[†] University Mainz.
[‡] Max-Planck-Institute of Polymer Research.

10.1021/ma801954y CCC: $40.75
Published on Web 12/09/2008

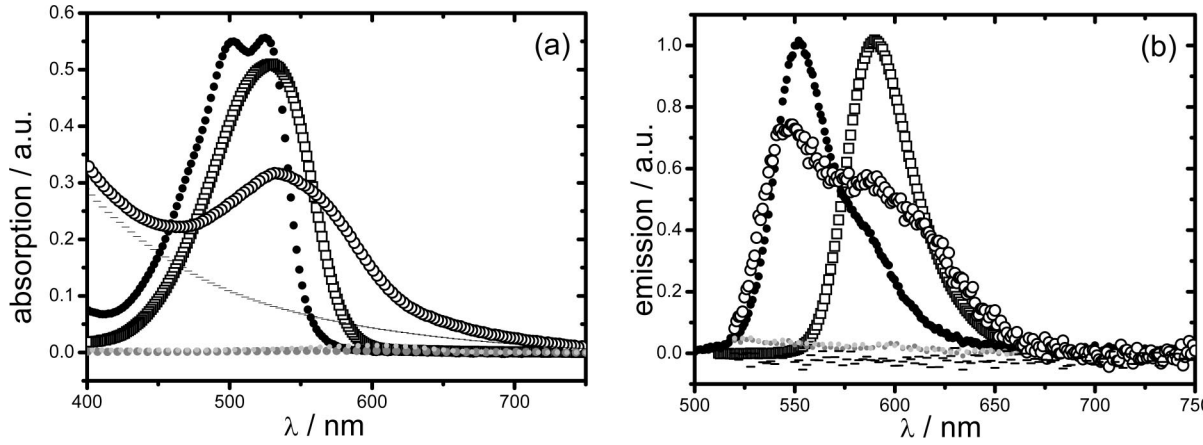

Figure 1. (a) Absorption and (b) emission spectra of Nile Red (NR) in THF (squares), NR loaded vesicles P_VC_NR13 (circles), blank vesicles P_VC36 (dashed line), Blind1 (dark gray dots), Blind2 (light gray dots), and NR in polybutadiene (black dots).

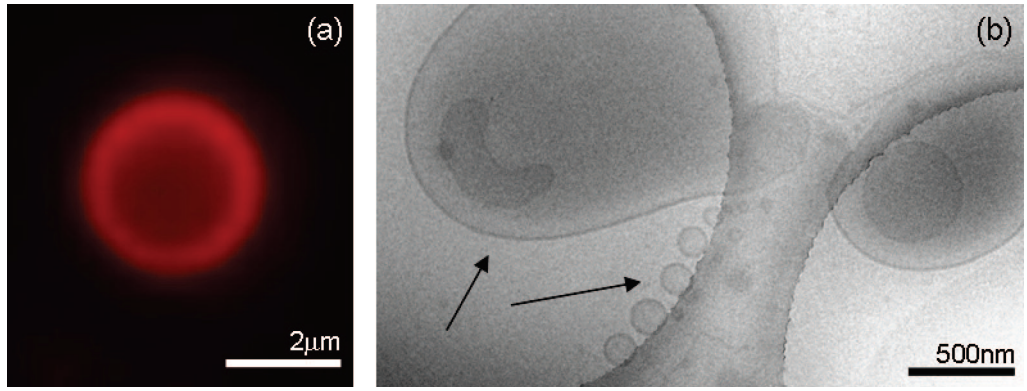

Figure 2. (a) Fluorescence microscopy image of Nile Red loaded vesicle in aqueous solution (true color) and (b) cryogenic TEM image of the very same solution P_VR_NR2 with its broad size distribution (arrows mark huge and small vesicles).

at $\lambda = 600$ nm. The diameter of the spherical particles was determined by TEM imaging to be 5.7 nm in dried state with a standard deviation of 0.6 nm.

Methods. Transmission electron microscopy imaging was performed at a FEI Tecnai 12 on carbon-coated copper grids. Cryogenic TEM imaging was done under liquid N_2 cryo conditions on holey carbon-coated copper grids. The microscope was used with 120 kV acceleration voltage, and the images were taken with a CCD camera.

Fluorescence correlation spectroscopy was performed with a commercial FCS setup (Zeiss, Germany) consisting of the module ConfoCor 2 and an inverted microscope model Axiovert 200. A Zeiss C-Apochromat 40×/1.2 W water immersion objective was used. The fluorophores were excited by a HeNe laser at $\lambda = 543$ nm, and emission was collected after filtering with a LP560 long pass filter. For detection, avalanche photodiodes were used to enable single-photon counting. An eight-well, polystyrene-chambered coverglass (Laboratory-Tek, Nalge Nunc International) was used as sample cell.

From the measured temporal fluctuations of the fluorescence intensity, $\delta I(t)$, an autocorrelation function

$$G(\tau) = 1 + \frac{\langle \delta I(t)\delta I(t+\tau)\rangle}{\langle I(t)\rangle^2} \quad (1)$$

corresponding to the probability that a chromophore inside the volume V at time t will still be inside at time $(t + \tau)$ can be evaluated. For an ensemble of freely diffusing fluorescence species the autocorrelation function has the following analytical form:[31]

$$G(\tau) = 1 + \frac{1}{N^*}\left(1 + \frac{\tau}{\tau_D}\right)^{-1}\left(1 + \frac{\tau}{S^2\tau_D}\right)^{-1/2} \quad (2)$$

where N^* is the average number of fluorescent molecules in the observation volume V, τ_D is the lateral diffusion time that a molecule stays in this volume, and $S = z_0/r_0$ is the ratio of axial to radial dimensions of V ($S \approx 6$ in our experiment). Furthermore, the diffusion time τ_D is related to the diffusion coefficient D of the species through $D = (r_0^2 + R_h^2)/4\tau_D$,[31] where R_h is the hydrodynamic radius, which for spherical particles is given by the Stokes−Einstein relation: $R_h = k_B T/6\Pi\eta D$, where k_B is the Boltzmann constant, T is the temperature, and η is the viscosity of the solution.[31] The calibration of the confocal observation volume was done using a reference standard with known diffusion coefficient, in our case orange fluorescent carboxylate-modified microspheres (FluoSpheres, Invitrogen) with a hydrodynamic radius of 54 nm (as obtained by dynamic light scattering).

Fluorescence microscopy imaging was performed at an Axio Imager A1 microscope (Zeiss, Germany), equipped with a 100× water objective (Zeiss) and a Texas Red filter set, $\lambda_{ex} = 560$ nm, $\lambda_{em} = 624$ nm with a green-red dichroic plate (Edmund Optics, Germany). Color pictures were taken using a Canon camera.

Absorption spectroscopy was performed using a V-650 UV/vis spectrophotometer (Jasco, Germany) with double-beam, photomultiplier tube detector, and external temperature control.

Fluorescence spectroscopy was performed using a FP-6500 spectrofluorometer (Jasco, Germany) with external temperature control.

Dynamic light scattering was performed with a Spectra-Physics SP2080 argon ion laser ($\lambda = 514$ nm), an ALV-SP125 goniometer with single photon detector SO-SIPD, and an ALV-5000 Multiple-Tau digital correlator or with a JDS Uniphase helium−neon laser ($\lambda = 623.8$ nm), an ALV-SP-86#060 goniometer with Avalanche photodiodes, and an ALV-3000 digital correlator. Angle-dependent measurements were carried out between 30° and 150° in steps of

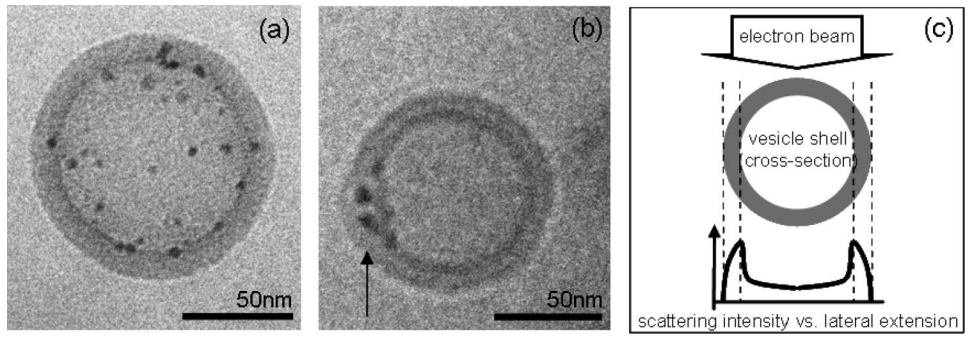

Figure 3. (a, b) Cryogenic TEM images of quantum dots-loaded vesicles P_VR_QD6 in aqueous solution. (c) Schematic drawing: TEM scattering intensity vs lateral extension.

20° at a temperature of 20 °C. Data evaluation was done according to the literature.[32]

Procedure. Vesicle solutions were produced following two different routes.

Cosolvent Method: Small vesicles with narrow size distribution were obtained starting with a copolymer solution in THF and dropwise addition of water. Controlled by a syringe pump (Bioblock Scientific), the dropping velocity of water addition was set to 9.9 mL/h. At ~30 wt % THF content the water addition was stopped, and the THF evaporated within 2−3 days. Standard final polymer concentration was $c_p = 1$ g/L in water. The samples were filtered through 0.45 μm filters (LCR, Millipore) before proceeding. Nile Red loading of those vesicles was achieved by the addition of dye to the starting copolymer/THF solution with different dye/copolymer weight ratios. Further treatment was done the same way.

Rehydration Method: Huge vesicles with broad size distribution were obtained starting with a copolymer solution in THF or chloroform and creating a film in a Teflon vessel. After film drying at 50 °C under vacuum, water was added. Film rehydration was supported by intense ultrasonic use and an elevated temperature of 50 °C. The samples were filtered through 5 μm (LS, Millipore) before proceeding. For DLS and FCS measurements, additional filtration through 0.45 μm filters (LCR, Millipore) was used to remove dust and larger structures. Nile Red loading of those vesicles was achieved by the addition of dye to the starting copolymer/THF solution. Therefore, the film consists of a dye/copolymer mixture with weight ratio of 1/20. Quantum dot loading of those vesicles was achieved by the addition of quantum dots to the starting copolymer/chloroform solution. Therefore, the film consists of a (quantum dots)/copolymer mixture with weight ratio 1/2.8, corresponding to a molar ratio of 1/600. The rehydration procedure was performed as described before.

Results and Discussion

The encapsulation of hydrophobic substrates into the hydrophobic inner membrane core of PB_{130}-*b*-PEO_{66} vesicles was realized for two model substrates with molecular size and a size of ~6 nm.

In order to study the potential influence of the surrounding polarity on the optical properties of an encapsulated hydrophobic dye, the hydrophobic dye Nile Red (NR) was employed to load vesicles via the "cosolvent method" starting from a solution of PB-*b*-PEO copolymer and NR in THF and dropwise water addition as described above. This leads to homogeneous colored vesicle solutions with average hydrodynamic radii in the range of 40−50 nm (sample P_VC_NR). The uptake of NR is in the range of 500−550 dye molecules per vesicle, as determined from absorption spectra after calibration with NR solutions in polybutadiene. This corresponds to an uptake of 3 mg of NR per 1 g of copolymer and therefore an encapsulation efficiency of 5 wt %. Blank vesicle samples without NR addition were prepared the same way (sample P_VC). Dynamic light scattering measurements showed no differences in size or size distribution of the vesicles with or without Nile Red, and cryogenic TEM images proved the vesicular structure for both cases (see Supporting Information). Analogous to this P_VC_NR vesicle sample, blind samples with no copolymer (Blind1) or PEO polymer with $M_W = 3500$ g/mol (Blind2) were prepared.

Figure 1 shows absorption and emission spectra for the samples. For $\lambda < 500$ nm the vesicle samples scatter light increasingly with decreasing wavelengths due to their particle size (see blank vesicle sample). The two blind samples with no copolymer or PEO polymer show no absorption or emission signal, respectively, thereby indicating no Nile Red uptake. In none of the samples can a fluorescence band at $\lambda_{max} = 660$ nm originating from NR in aqueous environment[33] be found. The emission maximum of NR in the vesicle is very close to the value found for NR in a PB film (Figure 1b), indicating its incorporation into the PB shell. As suggested by comparison with the NR emission in THF, the increased emission intensity of NR in the vesicle around 600 nm might be attributed to traces of THF remaining in the hydrophobic shell from preparation, but more likely are contributions of NR molecules located close to the hydrophobic−hydrophilic interface (see Supporting Information), which demonstrates the capability to probe the local environment in addition to the already reported loading properties described in e.g. ref 19.

For further investigations, starting from a dried copolymer and Nile Red film as described above, NR-loaded vesicles were prepared via the "rehydration method" (sample P_VR_NR). This method leads to vesicles with very broad size distribution and diameters ranging from 60 nm up to 3 μm. By fluorescence microscopy imaging of those huge fluorescent vesicles, the structure can be visualized. Figure 2a shows the image of a NR-loaded vesicle with a size of about 3 μm. The high fluorescence intensity at the outer shell supports the model of the hydrophobic loading into the vesicle shell and the unloaded, water-filled core. The exact position inside the shells inner membrane core or at the hydrophobic−hydrophilic interface cannot be determined here. Vesicles with diameters smaller than 2 μm appear as nearly homogeneously fluorescing spots due to resolution limits of the microscope. Cryogenic TEM imaging of the very same solution showed vesicles over the full size distribution, as expected and exemplarily seen in Figure 2b. In cryogenic TEM imaging vitrified water films are typically 100−200 nm thick. Huge vesicles with diameters of several micrometers lie only partly in those films and can therefore distort from their spherical shape in solution as obvious in Figure 2b.

The encapsulation of a larger hydrophobic model substrate was successfully realized utilizing highly fluorescent quantum dots (QD). The enclosing of these nanoparticles inside the PB-*b*-PEO vesicles was performed only via the film rehydration procedure, as the quantum dots solvent chloroform is immiscible

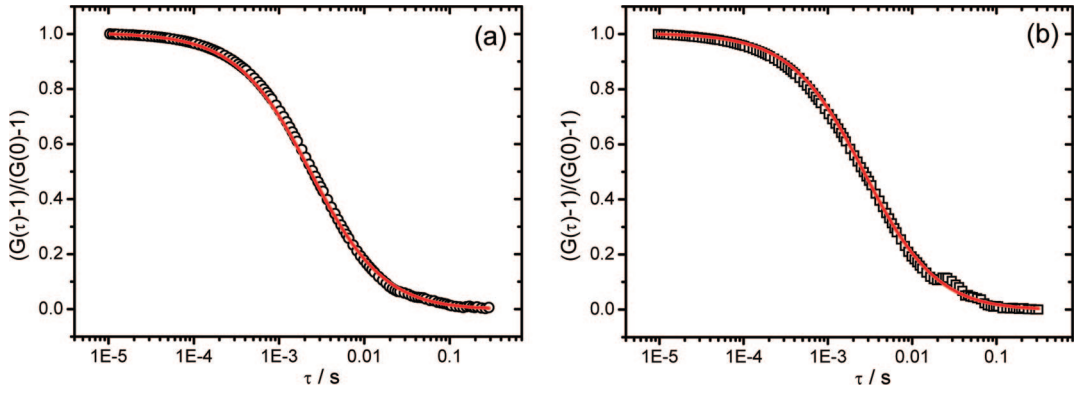

Figure 4. Normalized FCS autocorrelation curves (symbols) and corresponding fits with eq 2 (lines) for (a) FluoSpheres standards to determine the confocal volume (b) quantum dots-loaded vesicles P_VR_QD6.

with water and therefore not suitable for the cosolvent method. The rehydration procedure was done analogous to the Nile Red samples, but afterward filtration through 0.45 μm filters (LCR, Millipore) ensured a smaller vesicle size regime important for further characterization (sample P_VR_QD). Absorption and emission spectra indicated the presence of quantum dots in the vesicle solution after filtration (see Supporting Information). The quantification of QD load in the vesicles was so far not possible, as the rehydration method never led to a complete solution of material and the QD absorption peak is drowned in the high scattering background of those huge and broadly distributed vesicles. Furthermore, exact reference concentrations are difficult to determine for core/shell QD solutions.

Cryogenic TEM images of quantum dots containing vesicle sample P_VR_QD6 are shown in Figure 3. The PB-*b*-PEO copolymer exhibits a low scattering contrast compared to the quantum dots, enabling the quantum dots to be clearly seen as dark spots inside the vesicle structure. The TEM image represents a projection of the three-dimensional loaded vesicle (as it is frozen in the water film) into the two-dimensional imaging plane. Those quantum dots appearing in the inner core due to the projection are therefore also enclosed in the vesicle shell (see scheme shown in Figure 3c). Appropriate sample tilt during imaging reveals the quantum dots position in the middle of the vesicle shell (as can be seen in Figure 3b), thus in between the two polybutadiene layers, introducing a curvature into the assembled shell. This QD/PB-*b*-PEO system is an example of hydrophobic vesicle shell loading, with only hydrophobic interactions between copolymer and substrate addressed, and the phenomenon of bending around the guest particle is currently under investigation as a function of membrane thickness and incorporated nanoparticle diameters. A comparable mechanism has been observed experimentally and theoretically for the incorporation of colloids into block copolymers in the bulk.[34−36]

As cryogenic TEM imaging is not necessarily representing the entire sample, fluorescence correlation spectroscopy (FCS) measurements were performed additionally for measuring diffusion coefficients of fluorescent particles.[31,37−39] The observation volume in FCS strongly depends on the imaging optics and cannot be measured directly; therefore, suitable calibration procedures have to be applied first. Calibration in aqueous environment typically relies on the measurement of the characteristic diffusion time of a dye molecule with known diffusion coefficient, i.e., rhodamine 6G.[31] As the Nile Red-loaded as well as the quantum dots-loaded vesicles show a very much different fluorescence brightness compared to rhodamine 6G, we used commercially available fluorescently labeled polymer beads (FluoSpheres standards, Invitrogen) with a size and a brightness similar to those of the vesicles to calibrate our FCS setup. The average hydrodynamic radius of those standards was measured previously by angle-dependent dynamic light scattering, giving $\langle R_h \rangle = 54$ nm (biexponential fit and $q = 0$ extrapolation[32]) with an expected narrow size distribution (cumulant method,[32,40] normalized $\mu_2 \approx 0.05$ at 90° scattering angle, corresponding to a $\sigma_D = 0.22$ that is a polydispersity in radius of 25%). The important equations for FCS data evaluation are mentioned in the Experimental Section.

Table 1. Hydrodynamic Radii: FCS Results Compared to DLS Results[a]

	FCS			DLS	
sample	$\tau_D/\mu s$	$D_{22\,°C}/cm^2/s$	R_h/nm	$D_{20\,°C}/cm^2/s$	R_h/nm
FluoSpheres	2368			3.93×10^{-8}	54
P_VR_QD6	2750	3.68×10^{-8}	62	3.18×10^{-8}	67
P_VC_NR13	1626	5.82×10^{-8}	39	5.01×10^{-8}	43

[a] τ_D is the diffusion time obtained from FCS fit procedure, D_{FCS} is the diffusion coefficient related to FluoSpheres standards, and D_{DLS} diffusion coefficient is obtained from the biexponential fit procedure and extrapolation to $q = 0$.

In Figure 4, the experimentally obtained correlation functions and fits to the data using eq 2 are shown for the FluoSphere standards and the quantum dots loaded vesicles (P_VR_QD6). The data could be fitted reasonably well for the full correlation time regime spanning over more than 4 decades. The hydrodynamic radii of the loaded vesicles evaluated using the above FCS calibration procedure and the Stokes−Einstein relation are shown in Table 1. Results of dynamic light scattering (DLS) measurements of the same solutions are shown in Table 1 as well. The experimental angle-dependent DLS data were evaluated by biexponential fitting and $q = 0$ extrapolation as reported in the literature.[32] As light scattering averages the whole sample content and yields comparable particle sizes as FCS which averages only the fluorescent sample content (in our case the loaded vesicles), and comparable results are observed with the cryogenic TEM (two images exemplarily shown in Figure 3), the nice agreement of the independent methods allows to conclude the successful hydrophobic vesicle loading for the Nile Red as well as for the quantum dots system.

Conclusion

The hydrophobic shell of poly(butadiene)-*b*-poly(ethylene oxide) vesicles was successfully loaded with the fluorescent dye Nile Red and highly fluorescent quantum dots as hydrophobic model substrates. Fluorescence correlation spectroscopy measurements showed that fluorescing signals belong to the diffusion of fluorescently loaded vesicles only, demonstrating that no other aggregation or structure stabilization occurred. Cryogenic TEM and fluorescence microscopy imaging confirmed that the hydrophobic substrates were enclosed inside the hydrophobic vesicle shell. In case of the quantum dots loaded vesicles it has

been possible by cryogenic TEM imaging to prove that the QD are located in between the two hydrophobic poly(butadiene) layers of the shell bilayer, introducing curvature of the copolymer layers around the guest particles. The combination of independent methods of characterization made it possible to successfully investigate the localization of the hydrophobic substrates within the hydrophobic shell of the vesicles. Further experiments with differently sized quantum dots will determine the limits for particle enclosing inside the shell, revealing how far the double-layer can curve before different structural assemblies are favored.

Acknowledgment. We thank Prof. M. Schmidt, University Mainz, for the laboratory environment, him and Dr. W. Schärtl, University Mainz, for helpful discussions, M. Wagner, University Mainz, for the quantum dots synthesis, and Dr. U. Kolb and the "Elektronen Microscopie Zentrum" Mainz. For financial support we gratefully acknowledge Deutsche Forschungsgemeinschaft DFG (SFB 625), Fonds der Chemischen Industrie (FCI), and Polymat "Polymers in Advanced Materials" Mainz.

Supporting Information Available: Absorption and emission spectra, FCS and DLS data, cryogenic TEM images. This material is available free of charge via the Internet at http://pubs.acs.org.

References and Notes

(1) Discher, D. E.; Eisenberg, A. *Science* **2002**, *297*, 967–973.
(2) Lee, J. C.-M.; Bermudez, H.; Discher, B. M.; Sheehan, M. A.; Won, Y.-Y.; Bates, F. S.; Discher, D. E. *Biotechnol. Bioeng.* **2001**, *73*, 135–145.
(3) Förster, S.; Berton, B.; Hentze, H.-P.; Krämer, E.; Antonietti, M.; Lindner, P. *Macromolecules* **2001**, *34*, 4610–4623.
(4) Antonietti, M.; Förster, S. *Adv. Mater.* **2003**, *15*, 1323–1333.
(5) Jain, S.; Bates, F. S. *Science* **2003**, *300*, 460–464.
(6) Maskos, M. *Polymer* **2006**, *47*, 1172–1178.
(7) Caliceti, P.; Veronese, F. M. *Adv. Drug Delivery Rev.* **2003**, *55*, 1261–1277.
(8) Haag, R. *Angew. Chem.* **2004**, *116*, 280–284.
(9) Bermudez, H.; Brannan, A. K.; Hammer, D. A.; Bates, F. S.; Discher, D. E. *Macromolecules* **2002**, *35*, 8203–8208.
(10) Maskos, M.; Harris, J. R. *Macromol. Rapid Commun.* **2001**, *22*, 271–273.
(11) Jofre, A.; Hutchison, J. B.; Kishore, R.; Locascio, L. E.; Helmerson, K. *J. Phys. Chem. B* **2007**, *111*, 5162–5166.
(12) Chécot, F.; Lecommandoux, S.; Klok, H.-A.; Gnanou, Y. *Eur. Phys. J. E* **2003**, *10*, 25–35.
(13) Allen, C.; Maysinger, D.; Eisenberg, A. *Colloids Surf., B* **1999**, *16*, 3–27.
(14) Katakoa, K.; Harada, A.; Nagasaki, Y. *Adv. Drug Delivery Rev.* **2001**, *47*, 113–131.
(15) Choucair, A.; Soo, P. L.; Eisenberg, A. *Langmuir* **2005**, *21*, 9308–9313.
(16) Borchert, U.; Lippbrandt, U.; Bilang, M.; Kimpfler, A.; Rank, A.; Pescka-Süss, R.; Schubert, R.; Lindner, P.; Förster, S. *Langmuir* **2006**, *22*, 5843–5847.
(17) Lecommandoux, S.; Sandre, O.; Chécot, F.; Rodriguez-Hernandes, J.; Perzynski, R. *Adv. Mater.* **2005**, *17*, 712–718.
(18) Krack, M.; Hohenberg, H.; Kornowski, A.; Lindner, P.; Weller, H.; Förster, S. *J. Am. Chem. Soc.* **2008**, *130*, 7315–7320.
(19) Ghoroghchian, P. P.; Lin, J. J.; Brannon, A. K.; Frail, P. R.; Bates, F. S.; Therien, M. J.; Hammer, D. A. *Soft Matter* **2006**, *2*, 973–980.
(20) Nardin, C.; Thoeni, S.; Widmer, J.; Winterhalter, M.; Meier, W. *Chem. Commun.* **2000**, 1433–1434.
(21) Binder, W. H.; Sachsenhofer, R.; Farnik, D.; Blaas, D. *Phys. Chem. Chem. Phys.* **2007**, *9*, 6435–6441.
(22) Binder, W. H.; Sachsenhofer, R. *Macromol. Rapid Commun.* **2008**, *29*, 1097–1103.
(23) Lecommandoux, S.; Sandre, O.; Chécot, F.; Perzynski, R. *Prog. Solid State Chem.* **2006**, *34*, 171–179.
(24) Ghoroghchian, P. P.; Frail, P. R.; Susumo, K.; Park, T. H.; Wu, S. P.; Uyeda, H. T.; Hammer, D. A.; Therien, M. J. *J. Am. Chem. Soc.* **2005**, *127*, 15388–15390.
(25) Bockstaller, M. R.; Lapetnikov, Y.; Margel, S.; Thomas, E. L. *J. Am. Chem. Soc.* **2003**, *125*, 5276–5277.
(26) Chiu, J. J.; Kim, B. J.; Kramer, E. J.; Pine, D. J. *J. Am. Chem. Soc.* **2005**, *127*, 5036–5037.
(27) Ahmed, F.; Pakunlu, R. I.; Brannan, A.; Bates, F.; Minko, T.; Discher, D. E. *J. Controlled Release* **2006**, *116*, 150–158.
(28) Krishna, M. M. G. *J. Phys. Chem. A* **1999**, *103*, 3589–3595.
(29) Hines, M. A.; Guyot-Sionnest, P. *J. Phys. Chem.* **1996**, *100*, 468–471.
(30) Xie, R.; Kolb, U.; Li, J.; Basché, T.; Mews, A. *J. Am. Chem. Soc.* **2005**, *127*, 7480–7488.
(31) Rigler, R.; Elson, E. *Fluorescence Correlation Spectroscopy: Theory and Applications*; Springer-Verlag: Berlin, 2001.
(32) Schmidt, M. *Dynamic Light Scattering*; Brown, W., Ed.; Clarendon Press: Oxford, 1993; Chapter 8.
(33) Goodwin, A. P.; Mynar, J. L.; Ma, Y.; Fleming, G. R.; Fréchet, J. M. J. *J. Am. Chem. Soc.* **2005**, *127*, 9952–9953.
(34) Chiu, J. J.; Kim, B. J.; Yi, G.-R.; Bang, J.; Kramer, E. J.; Pine, D. J. *Macromolecules* **2007**, *40*, 3361–3365.
(35) Matsen, M. W.; Thompson, R. B. *Macromolecules* **2008**, *41*, 1853–1860.
(36) Kang, H.; Detcheverry, F. A.; Mangham, A. N.; Stoykovich, M. P.; Daoulas, K.Ch.; Müller, M.; de Pablo, J. J.; Nealey, P. F. *Phys. Rev. Lett.* **2008**, *100*, 148303.
(37) Haustin, E.; Schwille, P. *Curr. Opin. Struct. Biol.* **2004**, *14*, 531–540.
(38) Koynov, K.; Mihov, G.; Mondeshki, M.; Moon, C.; Spiess, W.; Müllen, K.; Butt, H.-J.; Floudas, G. *Biomacromolecules* **2007**, *8*, 1745–1750.
(39) Yin, M.; Sorokina, K.; Kuhlmann, C.; Li, C.; Mihov, G.; Koynov, K.; Luhmann, H.; Klapper, M.; Müllen, K.; Weil, T. *Biomacromolecules* **2008**, *9*, 1381–1389.
(40) Brown, J. C.; Pusey, N. *J. Chem. Phys.* **1975**, *62*, 1136–1144.

MA801954Y